Experimental analysis of the flow pattern of a pump turbine model in pump mode

Mark Guggenberger[1], Florian Senn[1], Helmut Jaberg[1]

Arno Gehrer[2], Manfred Sallaberger[3], Christian Widmer[3]

[1] Graz University of Technology, Austria
[2] Andritz Hydro, Austria
[3] Andritz Hydro, Switzerland

e-mail: mark.guggenberger@tugraz.at

Abstract. Reversible pump turbines are the only means to store primary energy in an highly efficient way. Within a short time their operation can be switched between the different operational regimes thus enhancing the stabilization of the electric grid. These qualities in combination with the operation even at off-design conditions offer a high flexibility to the energy market. However, pump turbines pass through operational regimes where their behaviour becomes unstable. One of these effects occurs when the flowrate is decreased continuously down to a minimum. This point is the physical limitation of the pump operation and is very difficult to predict properly by numerical design without a model test. The purpose of the present study is to identify the fluid mechanical phenomena leading to the occurrence of instabilities of pump turbines in pump mode. A reduced scale model of a ANDRITZ pump turbine was installed on a 4-quadrant test rig for the experimental investigation of unstable conditions in pump mode. The performed measurements are based on the IEC60193-standard. Characteristic measurements at a single guide vane opening were carried out to get a detailed insight into the instabilities in pump mode. The interaction between runner and guide vane was analysed by Particle Image Velocimetry. Furthermore, high-speed visualizations of the suction side part load flow and the suction recirculation were performed. Like never before the flow pattern in the draft tube cone became visible with the help of a high-speed camera by intentionally caused cavitation effects which allow a qualitative view on the flow pattern in the draft tube cone. Suction recirculation is observed in form of single vortices separating from each runner blade and stretching into the draft tube against the main flow direction. To find an explanation for the flow phenomena responsible for the appearance of the unstable head curve also characteristic velocity distributions on the pressure side were combined with high-speed visualizations on the suction side of the pump turbine model. The results enhance the comprehension of the physical background leading to the instability and improve the numerical predictability of the instability in pump mode.

1. Introduction

The characteristics of pump turbines operating in pump mode are well known to show instabilities at deliveries below the design flow rate. In pumps this distinct discontinuities in part load operation were proved to coincide with the beginning of flow separation at the impeller outlet [1]. Further research

found out that the instabilities lead to abrupt unsteady flow field changes and a loss of head in the pump characteristic [2]. Today it is still a challenge to predict the point by numerical simulations where the flow in a pump or a pump turbine is getting unstable and without the additional insight of a model test. In course of a design process numerical simulations have to prove themselves in everyday operation, often they are limited in complexity and computational resources. To improve the understanding and the numerical predictability of the flow inside pumps and pump turbines operating in deep part load several researches including constant temperature anemometry, transient pressure measurements, strain gauges, two-dimensional laser velocimetry or numerical simulations based on unsteady RANS turbulence modelling have been performed and reported [3, 4, 5]. However, the characteristics of the flow observed in the part load operating condition are not fully understood yet. For the purpose of understanding the physical background of the occurrence of the instability, visualizations play an important role. Investigations of a reduced scale model of a radial pump turbine, providing optical access for visualizations on the pressure side have been introduced recently [6]. The present study introduces an experimental analysis of the pump instability and extends the observation area by visualizations towards a transparent diffuser cone on the suction side of the model. The flow pattern in the draft tube cone became visible by using a high-speed camera. After describing the experimental setup, the measured phi-psi-characteristics are presented as well as the operation points investigated in the course of the PIV-measurements and the corresponding high-speed visualizations. Ensemble-averaging the PIV-results for different measurement planes at the pressure side in combination with detailed analysis of the high-speed visualizations describe the characteristics of the flow over the operation range in pump mode.

2. Experimental set up and pump turbine model investigated

A model of a reversible pump turbine of a specific speed of n_q=45 was under investigation in the closed-circuit 4-quadrant test rig at the laboratory of hydraulic fluid machinery at Graz University of Technology. The machine, exhibiting the instability in pump mode typical for all pump turbines at this specific speed, was equipped with a 200 kW motor-generator. It consists of a runner with 9 blades, a guide vane apparatus with 20 guide vanes and 10 stay vanes (Figure 1). A 500 kW centrifugal pump provides a maximum head of 90 m and a maximum discharge of 0.75 m^3s^{-1}. The experimental set up and the measurement instruments were based on the IEC60193 standard [7] providing measurement accuracy of ± 0.2% even at off-design operation points with low discharge.

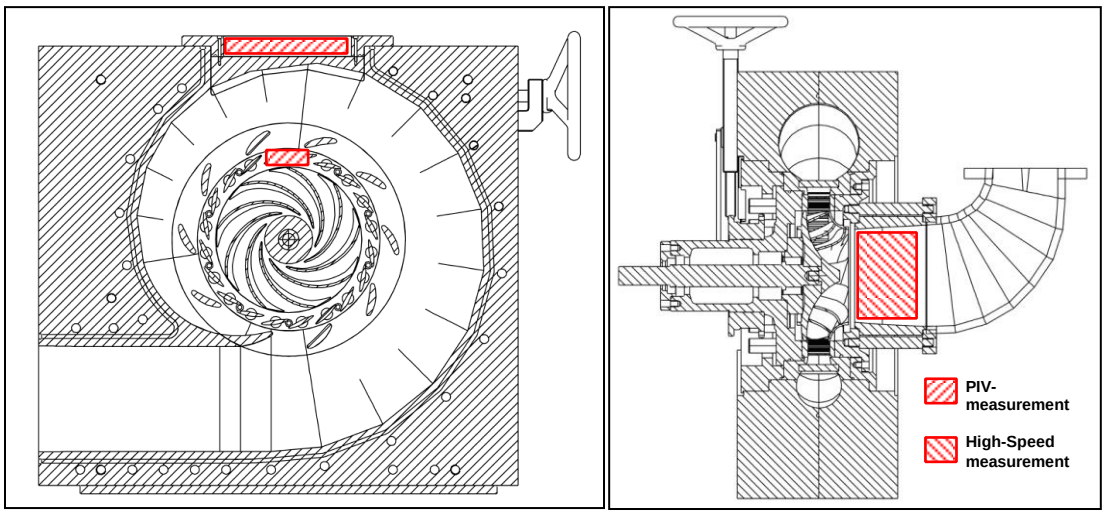

Figure 1. Reduced pump turbine model and investigation areas: (a) Front View, (b) Top View

To analyze the fluid dynamic mechanisms responsible for the appearance of the unstable behavior two-dimensional ensemble-averaged Particle Image Velocimetry (PIV) was applied to visualize the velocity field on the pressure side in the vaneless space between impeller and guide vanes. To implement this optical measurement method a modification of the casing around the pump turbine runner was necessary. To gain a radially oriented optical access to the area of interest a milled two-piece Aluminium-casing was equipped with an optical window made of acrylic glass (PMMA). Furthermore two guide vanes were also made of acrylic glass. For an axial view into the area between the guide vanes and the runner an additional window was integrated into the support ring of the guide vanes. Thus the model provided access for the measurement of velocity fields in one radial and three axial normal planes (Figure 2 (a)).

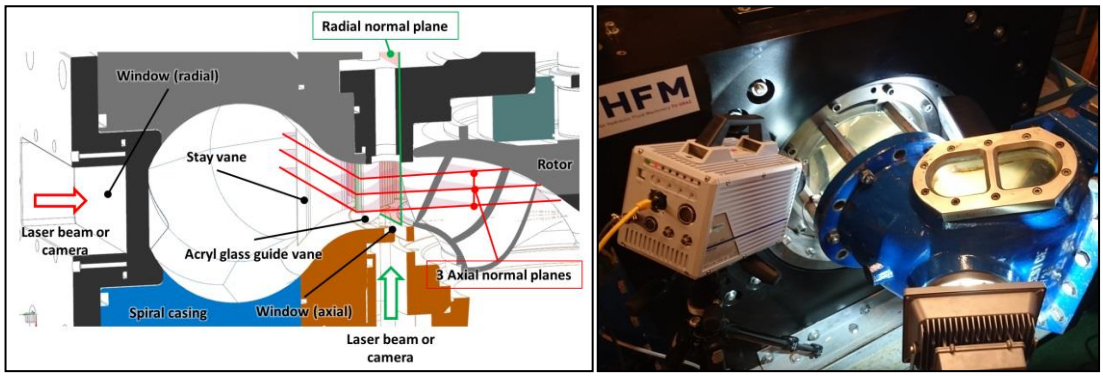

Figure 2. (a) Measurement planes; (b) experimental setup for high-speed visualizations

While the axial optical access allows the observation of the velocity field in a plane normal to the rotation axis of the rotor (either at 25%, 50% or 75% channel height), the radial optical access allows the observation of the velocity field in a plane tangential to the outer diameter of the rotor (D=0.35 m). A calibration target with a grid of points having a defined distance had to be placed exactly there where the laser light sheet was directed into the fluid flow to calibrate the camera system in a way that the real velocity of flow was determined. Figure 3 shows pictures taken in the radial (a) and axial (b) direction of view. The trailing edge and the pressure side of a runner blade are clearly visible on the left hand side looking straight through the acrylic glass guide vanes. The picture on the right hand side shows the axial direction of view. The dotted lines highlight the laser light planes investigated in course of the measurement program. The blurred and black areas needed to be masked in course of the PIV-evaluation process. For each operation point investigated by PIV 500 single velocity fields were created for one rotor-/ stator-position. An encoder was attached at the runner's axis to trigger the PIV-system with the runner position. In combination with 21 different rotor-/stator-positions one full blade channel was measured in the end. The result was a global velocity field consisting of 10500 single flow fields.

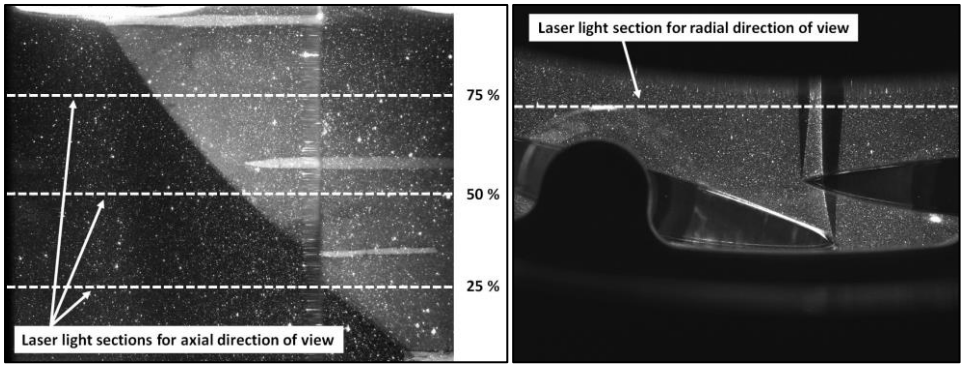

Figure 3. (a) Radial direction of view; (b) Axial direction of view

To perform a qualitative visualization of the flow on the suction side of the pump turbine model a high-speed camera system was used. Figure 2 (b) shows the arrangement of the equipment on the suction side of the model. The flow pattern in the draft tube cone were made visible by intentionally provoking cavitation through a low absolute pressure level in the test rig. The high-speed camera used for the visualization was a Photron Fastcam SA1.1 with a Nikon Nikkor 60mm F2.8 lens, 100 W LED headlights and the Photron FASTCAM Viewer Software.

3. Results

The characteristic curve was measured with a constant runner speed of 900 rpm (Figure 4). The discharge coefficient φ and energy coefficient ψ are defined by eq. (1). Four operation points (OP) were chosen for the laser-optical measurements on the pressure side of the model runner. OP1 was set in the local best efficiency point, OP2 and OP3 in the range of the instability and OP4 in deep part load. Following the numeration of the operation points the characteristic was measured from larger to smaller flow rate.

$$\varphi = \frac{Q}{\pi\omega(D/2)^3} \qquad \psi = \frac{2E}{(\omega D/2)^2} \tag{1}$$

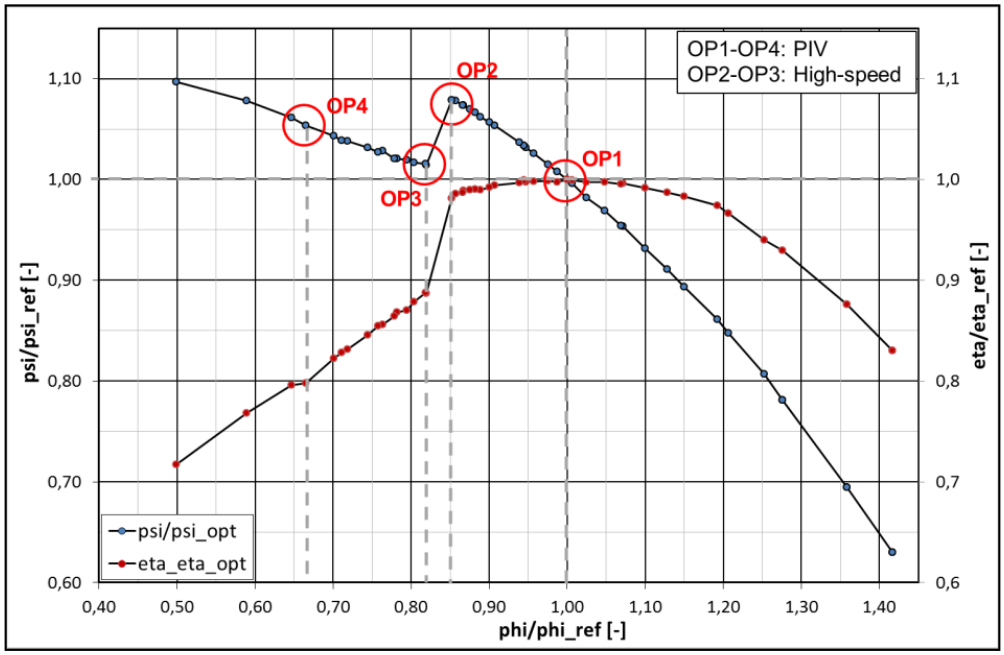

Figure 4. Operation points investigated in the course of the PIV-measurements and the high-speed visualizations

At a guide vane opening of 15° the operation of the pump turbine model became unstable at 85% of BEP flow rate. A head drop of about 6% occurs and a significant increase of vibrations and noise can be noticed. A variation of the runner speed between 900 and 1300 rpm as well as different values of the cavitation coefficient σ_{nD} (varied in a range of 0.2 to 1.0 and defined by eq. (2)) did not affect the instability. Although the operation points limiting the head drop are reliably reproducible, it was not possible to run a stable operation between the stable and instable branch.

$$\sigma_{nD} = \frac{NPSE}{n^2 D^2} \tag{2}$$

During the PIV-measurement campaign the cavitation coefficient σ_{nD} was kept at a constant level of 1 whereas the high-speed visualizations were recorded at a cavitation coefficient of 0.18. The operation points chosen for the qualitative visualizations are indicated in Figure 4. No cavitation was visible at all in the local best efficiency point even at a cavitation coefficient of 0.18. At the operation point in part load at 66% of BEP flow rate the cavitation in the draft tube cone massively increased and therefore made the visualizations impossible at smaller flow rates.

3.1. PIV-measurements of the flow pattern on the pressure side

The 10500 recorded velocity fields were averaged in order to obtain more valuable results and to separate the stochastically component from the mean value of the flow [8]. This averaging was done for each operating point, see eq. (3).

$$\bar{c}(\vec{x}) = \frac{1}{10500}\sum_{i=1}^{21}\sum_{j=1}^{500} c(\vec{x}, t_j) \tag{3}$$

The measured and averaged velocity field $\bar{c}(\vec{x})$ was normalized by the circumferential velocity u_1 at the outlet of the runner to allow a comparison of the PIV-results for different operation points, see eq. (4).

$$\bar{c}^{+} = \frac{\bar{c}(\vec{x})}{u_1} = \frac{2\,c(\vec{x})}{\omega D} \tag{4}$$

The velocity contour plots presented in Figure 5 show PIV-results for the four different operation points OP1 – OP4 at a guide vane position of 15°. While the y-axis represents the channel height of the runner, the x-axis refers to the extension of the blade channel in circumferential direction.

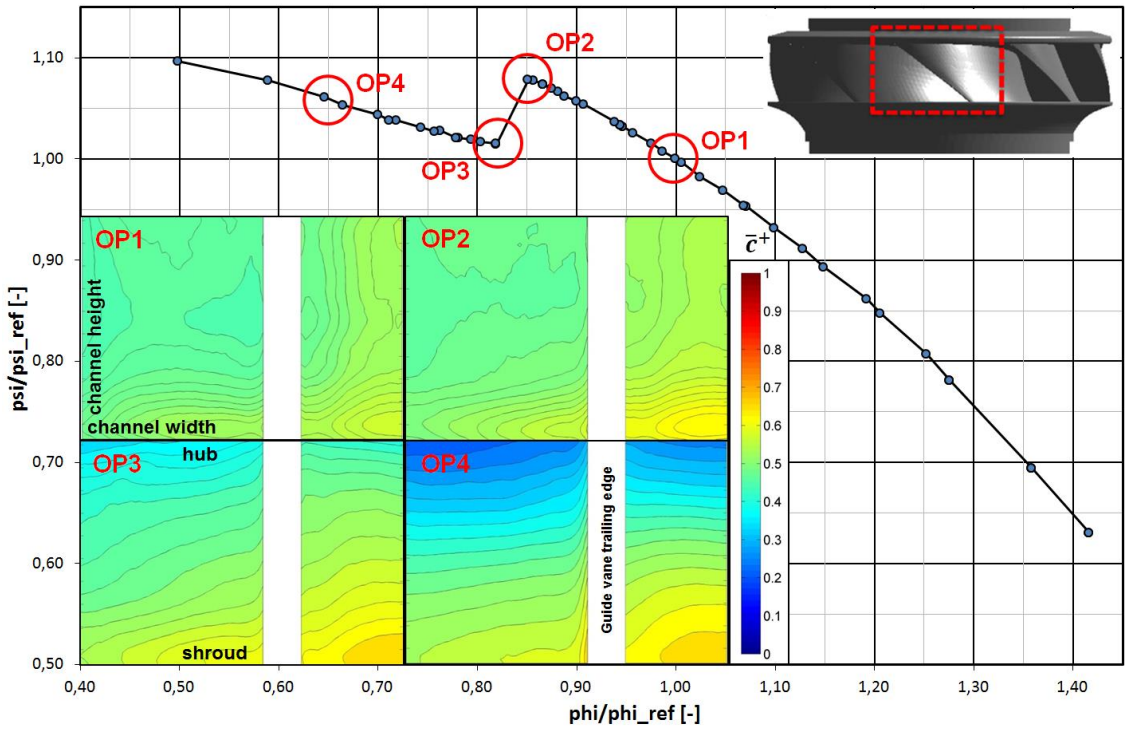

Figure 5. Globally averaged PIV-results at different operation points

The measurement result for the local best efficiency point (OP1) shows a widely homogenous velocity distribution over the whole blade channel. A slightly increased velocity distribution can be recognized at the shroud of the runner. This trend continues in operation point OP2. By further decreasing the discharge, the operation of the pump turbine model became unstable and suddenly the head drops (OP3).

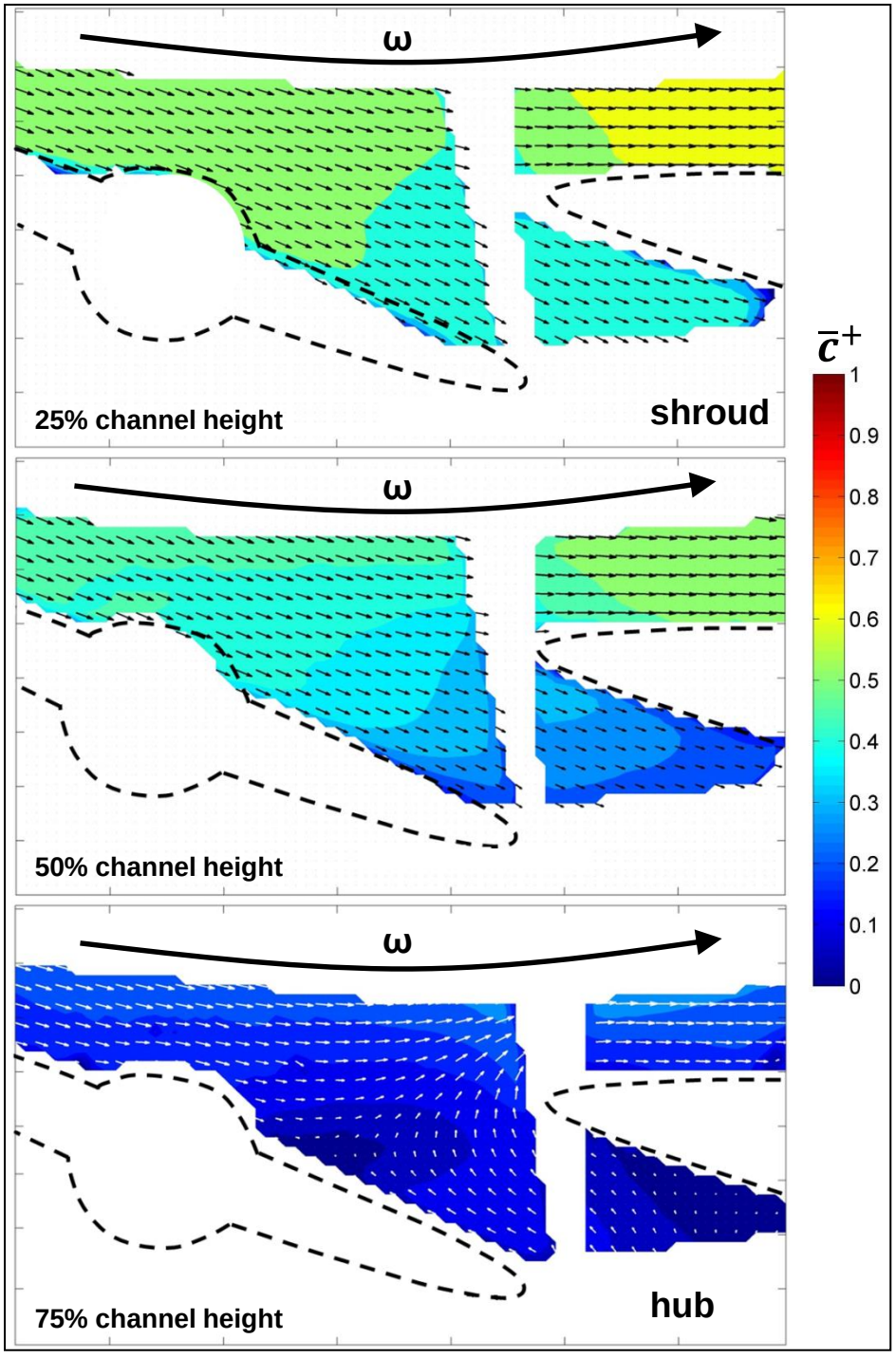

Figure 6. Averaged axial normal velocity contours showing back flow at OP4

Regarding the velocity distribution spread over the blade channel low values can be located near the hub and increasing to the shroud. In the operation point in deep part load (OP4) the velocity of the flow field decreases even more – indicated by a minimum normalized velocity of 0.25 at the hub and a maximum of 0.65 at the shroud of the runner. Although, compared to the local optimum point the total flow rate significantly decreased the velocity field near the shroud seems to be increased. The evaluation of globally averaged velocity contours allows to conclude, that for all investigated operation points at a guide vane position of 15° the velocity distribution is non-uniformly distributed in the vaneless space between the runner and the guide vanes. It is assumed, that the low velocity flow field is caused by the rotor-stator interaction. It is located from the hub to the mean of the blade channel in the vaneless space. This inhomogeneity gets stronger in the operation range where the head drop occurs and in deep part load.

The presented results refer to two dimensional PIV measurements carried out for a tangential normal plane in the radial direction of view. Therefore it is not possible to verify whether the inhomogeneous flow distribution indicates recirculation regions or not. This aspect can be examined with the results for the axial normal measurement plane for three channel heights. Figure 6 presents the results for the globally averaged axial normal measurement plane by superposing the velocity magnitude contours with the velocity vectors. The plots represent the results of the operation point in deep part load (OP 4) including a detailed view of a section. Also the direction of the runner and the guide vanes are sketched in the figure to allow a better understanding of the flow pattern. The results feature a good accordance of the single planes to each other. The visualization of the normalized velocity on the three different measurement planes for the axial direction of view enabled the detection and localisation of recirculation and back flow regions, respectively. At a channel height of 75% – located near the hub – back flow emerged. The recirculation spreads into the vaneless space having its source in the area of the guide vanes. At a channel height of 50% and 25% no back flow regions could be detected in this operating point when averaging the results of the blade channel. These results correspond to the measurement results of Hergt and Starke and also Schrader who related the head curve instability with a recirculation of the flow in the guide vane apparatus by which the resistance of the guide vanes increase all of a sudden [9, 10]. But it can also be shown [1] that the head curve instability under consideration coincides with a sudden change of the runner outflow even if there is no guide vane apparatus present and thus indicating that the cause for said instability might be the flow at the runner exit.

3.2. High-speed visualization of the flow pattern at the suction side

An extract of the records of the high-speed visualizations of the flow pattern at a cavitation coefficient of 0.18 at the suction side are presented in Figure 7. At the top of the figure the photographs illustrate flow pattern in the operating point limiting the stable operation range of the characteristic curve in part load (OP2). Strong but stable cavitation occurred on the leading edge and the suction side of the runner. The cavitation can be observed over a height of 50-60% of the leading edge and corresponds to a low incidence angle of the flow depending on the design of the impeller. A traveling bubble cavitation was recognized at the impeller throat, similar findings are made by Avellan et al. [11]. No cavitation was observed at the inlet of the runner coming from the leakage flow through the shroud gap and no suction recirculation is detectable yet. The photographs on the bottom of Figure 7 illustrate the flow on the suction side in the operating point directly after the head drop occurred. A part load flow recirculation at the inlet of the runner developed. The travelling bubble cavitation is no longer attached to the blade and extends into the draft tube cone. Single vortices occur in the outer diameter of the runner inlet separating from each runner blade and stretching into the draft tube against the main flow direction. The vortices rotated with a lower frequency (about 5 Hz) than the runner itself ($\omega = 15$ Hz). Because of their lower circumferential speed the runner blades cut them continuously. Additionally to the circumferential velocity they rotate around their own axis. The origin of the back flow vortices seemed to be in the blade channel. These findings agree with other results published in the literature [12] but are now visualized in this way for the first time.

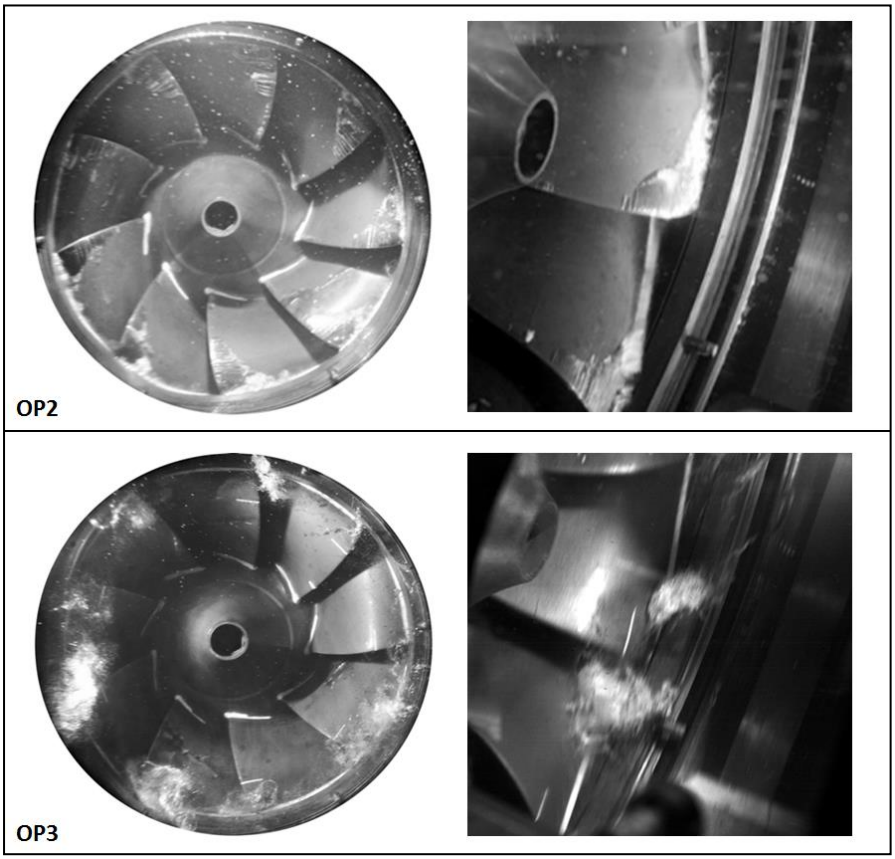

Figure 7. Visualization results of two different operating conditions, OP2 and OP3

For lower values of the flow rate the cavitation vortices extend even deeper into the draft tube cone against the main flow direction. Figure 8 should give a model representation of the flow pattern on the suction side in part load operation. While green colored vectors illustrate the main flow, the red colored recirculation zones extend into the draft tube cone and having their origin in the runner blade channels. As a result the helical vortex structures, colored in yellow, arise on the suction side of the model between the main flow and the backflow turning around its own axis.

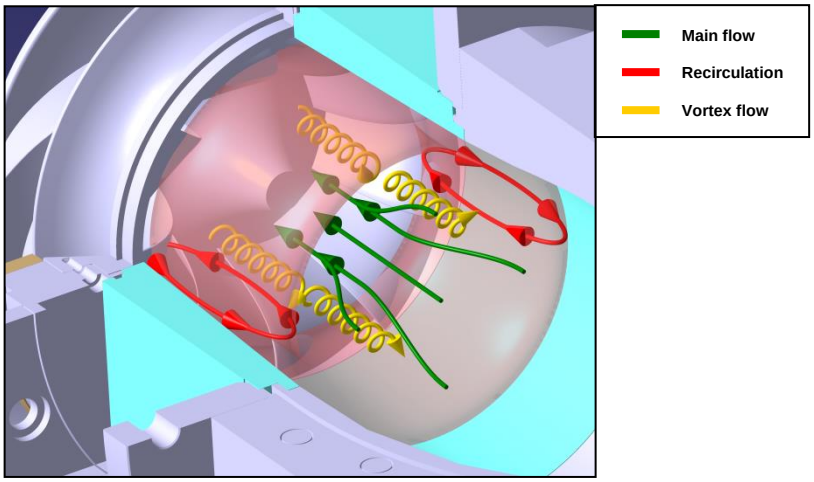

Figure 8. Model representation of the suction side flow pattern in part load operation

4. Conclusion

This paper presents the investigation of the flow pattern in a pump turbine model with two different visualization techniques. In the investigated operation points a non-uniform velocity distribution developed in the vaneless space between the guide vanes and the runner. While minimum values of the velocity distribution can be located near the hub, local maxima appeared near the shroud of the runner. The flow inhomogeneity got more distinctive in the operation range near head drop and in strong part load. Combining the results of the different measurement planes enabled the detection and localization of a back flow region. Flow recirculation was detected in the measurement plane at a blade channel height of 75% which was located near the hub of the runner. The back flow spreads into the vaneless space having its source in the area of the guide vanes. In the operation point directly when the head drop occurred, single vortices developed, separating from each runner blade and stretching into the draft tube against the main flow direction. The correlation of the head drop in the pump turbine characteristic with the vortex flow recirculation emerged simultaneously has to be investigated in more detail. So far, it is assumed that the an incorrect flow velocity incidence angle at the impeller inlet and cross sections too big for the discharge below the BEP lead to three-dimensional flow pattern and back flow at the impeller in- and outlet. The high speed visualization of the flow at the inlet of the runner indicates the necessity of further investigations to accurately survey its mechanism and dynamical characteristics.

Acknowledgments
The present study was carried out in the frame of the PT Instability project (FFG N° 846059), in a partnership with ANDRITZ. The authors would like to thank the Austrian Research Promotion Agency (FFG) for their financial support as well the ANDRITZ for their involvement and support. The authors would also like to thank Prof. Woisetschläger, Patrick Zeno Sterzinger and Stefan Leithner for their support with the Laser optical measurements.

Nomenclature

BEP	Best efficiency point
$\bar{c}$	Global averaged velocity field $[ms^{-1}]$
$\bar{c}^+$	Normalized velocity field $[-]$
D	Runner outlet diameter $[m]$
E	Specific hydraulic energy $[Jkg^{-1}]$
φ	Discharge coefficient, phi $[-]$
ψ	Energy coefficient , psi $[-]$
η	Efficiency, eta [%]
NPSE	Net Positive Suction Energy $[Jkg^{-1}]$
n	Runner speed $[s^{-1}]$
σ_{nD}	Cavitation coefficient
n_q	Specific speed $[rpm]$
Q	Discharge $[m^3s^{-1}]$
$\vec{x}$	Position vector $[m]$
t_j	Timestep j $[s]$
ω	Runner Angular Velocity $[rads^{-1}]$
u_1	Reference circumferential velocity $[ms^{-1}]$
$\vec{x}$	Position vector $[m]$

References

[1] Jaberg H and Hergt P 1989 Head curve stability in radial pumps *3. Joint ASCE/ASME Mechanics Conference (La Jolla, California)*
[2] Kaupert K 1997 Unsteady Flow Fields in a High Specific Speed Centrifugal Pump PhD Thesis *ETH Zürich*
[3] Stoffel B 1989 Experimentelle Untersuchung zur räumlichen und zeitlichen Struktur der Teillast-Rezikulation bei Kreiselpumpen *Forschung im Ingenieruwesen Vol 55*
[4] Braun O 2009 Part Load Flow in Radial Centrifugal Pumps *PhD Thesis EPFL*
[5] Berten S 2011 Experimental and Numerical Analysis of Pressure Pulsations and Mechanical Deformations in a Centrifugal Pump Impeller *ASME-JSME-KSME 2011 Joint Fluids Engineering Conference: Vol. 1 (Hamamatsu, Japan)*
[6] Guggenberger M, Senn F and Jaberg H 2015 Investigating the dynamic aspects of the turbine instability of a pump turbine model *Proceedings of the 6th IAHR International Meeting of the Workgroup on Cavitation and Dynamic Problems in Hydraulic Machinery and Systems (Ljubljana, Slovenia)*
[7] IEC60193 1999 Hydraulic turbines, storage pumps and pump-turbines – Model acceptance tests *Second edition 11-1999*
[8] Guggenberger M, Senn F, Schiffer J and Jaberg H 2014 Experimental investigation of the turbine instability of a pump-turbine during synchronization *27th IAHR Symposium Hydraulic Machinery and Systems (Montreal, Canada)*
[9] Hergt P and Starke J 1985 Flow Patterns Causing Instabilities in the Performance Curves of Cetrifugal Pumps with Vaned Diffusers 2. *Int. Pump Symposiom (Houston, Texas)*
[10] Schrader H 1939 Messungen an Leitschaufeln von Kreiselpumpen *PhD Thesis TU Braunschweig Würzburg-Aumühle: Triltsch*
[11] Avellan F 2004 Introdcution to cavitation in hydraulic machinery *6th International Conference on Hydraulic Machinery and Hydrodynamics (Timisoara, Romania)*
[12] Schiavello B and Sen M 1980 On the prediction of the reverse flow onset at the centrifugal pump inlet *ASME 22nd Annual Fluids Engineering Conference, (New Orleans, Louisiana)*